This is the Pre-Published Version.
M. Thomsen, C. Fernandez-Pello, X. Huang, S. Olson, P. Ferkul (2020) *Buoyancy Effect on Downward Flame Spread Over PMMA Cylinders*, Fire Technology, 56(1): 247–269. https://doi.org/10.1007/s10694-019-00866-0
This is a post-peer-review, pre-copyedit version of an article published in Fire Technology. The final authenticated version is available online at: https://doi.org/10.1007/s10694-019-00866-0.

Buoyancy effect on downward flame spread over PMMA cylinders

Maria Thomsen[1], Carlos Fernandez-Pello[1], Xinyan Huang[1,2], Sandra Olson[3] & Paul Ferkul[3]

[1]Department of Mechanical, Engineering, University of California, Berkeley, CA 94720, USA

[2]Department of Building Services Engineering, Hong Kong Polytechnic University, Hong Kong

[3]NASA Glenn Research Center, 21000, Brookpark Rd., Cleveland, OH 44135, USA

ABSTRACT

Understanding material flammability at different gravity levels is important for fire safety applications in space facilities where the environments may include microgravity, low velocity flows, low pressure and elevated oxygen concentration. One possible approach to simulate on-earth the burning behavior inside spacecraft environments, and facilitate testing, is to reduce buoyancy effects by decreasing ambient pressure. The objective of this work is to study the effect of pressure, and consequently buoyancy and indirectly gravity, on downward flame spread rate over cylindrical samples of polymethyl-methacrylate (PMMA), and by comparison with reduced gravity data, observe up to what point low-pressure can be used to replicate flame spread in space facilities. Experiments in normal gravity are conducted using pressures ranging between 100 and 30 kPa and oxygen concentrations between 19% and 23%, with a forced flow velocity of 100 mm/s. The low-pressure data is compared with microgravity data obtained aboard the International Space Station during the BASS-II experiments. Results show that reductions of ambient pressure slow down the flame spread process approaching that expected at low gravity. The normal gravity and microgravity data are correlated in terms of a mixed convection parameter that describes the main controlling mechanisms of heat transferred. Although the correlation works well for the normal gravity data it does not work as well for the microgravity data. However, it provides information about what is to be expected in environments of variable ambient pressure, oxygen concentration, and reduced gravity, providing an insight for future designs when considering fire safety in spacecrafts.

KEYWORDS: Flame spread, microgravity, reduced pressure, oxygen concentration, PMMA

1 INTRODUCTION

Fire safety in spacecraft environments is an important concern for space travel [1–3] particularly because of the criticality of such an event. There are combustible materials in spacecraft cabins and space facilities, and also conditions that can ignite them and initiate a fire. Also, the fire risk will increase as the time spent in space is increased with the operation of proposed long space missions, and the establishment of facilities on the Moon and Mars. The flammability of solid combustible materials is a measure of their fire hazard, and consequently is often used to characterize the fire risk of a material. Flammability of a material is typically characterized by its ignitability, flame spread rate, heat release rate, and toxicity. The most effective fire safety strategy is to prevent ignition. However, once ignited, flame spread presents a significant safety risk to the space travel. Thus, experiments on flame spread are often used to determine the fire hazard of a material and the corresponding fire-extinguishing strategy [4].

A problem with testing on Earth the flammability of materials to be used in space facilities is that spacecraft/space facilities fire conditions are very different from those encountered on earth since they include microgravity, or reduced gravity, low velocity flows, and potentially low pressure (~60 kPa) and elevated oxygen concentration (~34%) [5]. The atmospheric conditions are referred to as space exploration atmospheres (SEA) and are designed to reduce preparation time for space walks, while keeping the partial pressure of

oxygen acceptable for human respiration (Normoxic conditions) [5,6]. Because of these environmental conditions, material burning may be very different in a space facility than on Earth. In a space facility, gravity is reduced (often to microgravity) and there are low-velocity flows that are of the order of 100 to 200 mm/s, due to the heating, ventilation and air conditioning (HVAC) system [1]. Such flows are significantly smaller than those induced by the flame-induced buoyancy flow in normal gravity (300 to 600 mm/s) [7]. A clear example of the flow effect on the burning of a solid fuel is that of Fig. 1 that shows a comparison of the flame characteristics between normal gravity and microgravity for a flame spreading over the surface of a PMMA rod under the same ambient pressure and oxygen concentration. In normal gravity (Fig. 1, left) buoyancy induces an upward gas flow that contracts and enlarges the flame, and affects the spread of the flame. In microgravity (Fig. 1, right) at a gas flow of 200 mm/s, the flame is rounder due to radial mass diffusion and bluer due to a lower temperature and soot concentration. Experimental studies of the combustion of solid fuels in spacecraft environments are very limited, primarily because of the difficulty of conducting the experiments [8–16] and the extensive time required to conduct them. Fire testing of materials to be used in space facilities requires either a reduced gravity facility, or alternative approaches to reduce buoyancy. However, ground-based microgravity facilities such as drop towers or parabolic flights are limited to a few second duration. Testing in a space-based facility is very expensive and limited in available space and opportunities. Thus, it is relevant to study the possibility of simulating reduced buoyancy material burning on earth, not only to reduce the cost of testing but also for model verification.

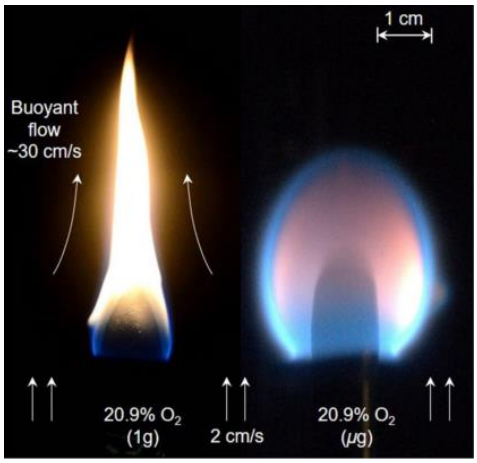

Figure 1. Photo of flames spreading over black PMMA rods in normal gravity (flame on the left) and microgravity (flame on the right) in air.

A possible approach to test flame spread and burning at different buoyancy levels is to vary the orientation of the solid surface where the flame spreads [17–26]. Two primary approaches have been followed, one is to change the angle of inclination of the solid surface [17–23] or to conduct the experiments in a ceiling configuration [24–26]. However, there are several problems with changing the surface orientation to reduce the effect of gravity; one is that the thickness of the boundary layer is changed and consequently the heat flux from the flame to the surface is also changed, ultimately affecting the flame spread rate [19,25]. Another is the stratification of the hot pyrolyzate near the solid surface in a ceiling orientation or away from the surface in a floor orientation that changes the transport of the pyrolyzate and air [18,26]. Thus, a more promising approach is to use reduced pressure, and consequently density, to reduce gravity effects. Several studies have taken advantage of the changes in buoyancy resulting from reducing pressure to simulate solid combustion (ignition, opposed flame spread, extinction) encountered in microgravity [27–32]. Since reducing buoyancy reduces the velocity of the gas flow induced by the flame, the effect of reducing the ambient pressure on the flame characteristics and the spread rate is similar to that of reducing the flow velocity. This is relevant because a constraint to reproducing flame spread in spacecraft environments in normal gravity is that the low flow velocities encountered in spacecraft (~100 to 200 mm/s) cannot be attained in normal gravity because the

buoyant flow (~300 to 600 mm/s) overwhelms the forced flow. Thus, flame spread and subsequent burning of a material in reduced gravity, low velocity flows, can be at least partially simulated in reduced pressure, low velocity flows.

This work presents experiments conducted to study the spread of flames over the surface of PMMA rods in an opposing gas flow in normal gravity as a function of the ambient pressure and the gas flow oxygen concentration. The tests are conducted with the samples vertical, such that the gravity vector is parallel to the sample centerline and the forced flow flowing upward (downward flame spread in an opposed forced flow). The results are analyzed and correlated in term of the mixed convective flow generated by the spreading flame in the presence of gravity and compared with microgravity experiments of opposed flame spread in a pure forced flow previously conducted in the ISS as a part of the Burning and Suppression of Solids-II (BASS-II) project [15,33,34]. The correlation of the results is also used to infer the flame spread behavior at different gravity levels.

2 EXPERIMENT

The samples used in all the experiments are made of cast black polymethyl methacrylate (PMMA). Sample length was 90 mm for the normal gravity tests and 57.2 mm for the microgravity tests. Sample diameters were 12.7, 9.5, and 6.4 mm (Fig. 2). The sample material and geometry were selected to compare the normal gravity results with the BASS-II microgravity experiments. In addition, PMMA is typical of non-charring thermo-plastics and has been widely used in the past because it has well determined properties and produces repeatable results. Also, PMMA is potentially going to be used in some components, such as windows, in future planned spacecrafts.

2.1 Normal gravity tests

The normal gravity experiments were conducted in an apparatus previously developed to study the flammability of solid combustible materials under varied ambient conditions [28]. The apparatus consists of a laboratory scale combustion tunnel that has a 125 mm by 125 mm cross section and is 600 mm in total length. The first section of the duct serves as a flow straightener while the other segment of the duct is used as the test section. The tunnel is inserted in a 105 L pressure chamber as shown in Fig. 3.

Figure 2. PMMA samples used in the normal gravity tests.

The chamber is provided with a flow system that provides constant supply and exhaust of gases to avoid vitiation problems. Compressed house air or nitrogen, and oxygen were supplied through critical nozzles (O'Keefe Controls) to the bottom of the duct while constantly evacuating to maintain constant the pressure inside the chamber. The chamber pressure was controlled by a high-capacity vacuum generator (Vaccon JS-300) and a mechanical vacuum regulator. The chamber pressure was monitored constantly with an electronic pressure transducer (Omega Engineering, Inc. PX303-015A5V). The tests were conducted at pressures ranging between

100 and 30 ± 2 kPa, with oxygen concentrations varied between 19% and 23% by volume. The forced flow velocity was fixed at 100 mm/s in all the tests. This flow velocity was selected because is the flow velocity that will be used in future microgravity tests as part of the SoFIE/MIST experiments to be conducted by NASA on board ISS, and that was selected because is similar to that induced by the HVAC in spacecraft.

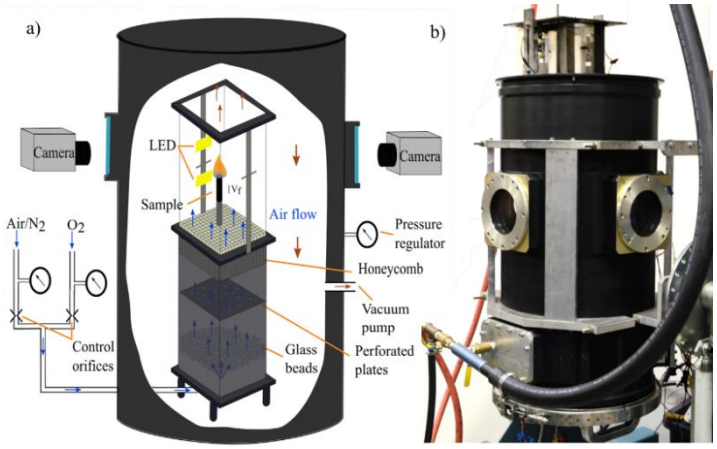

Figure 3. (a) Schematic of experimental apparatus and (b) photograph of the setup used in the normal gravity experiments.

During a test, the sample is placed vertically in the center of the test section, supported on a metal cylinder of the same diameter to prevent flow disturbances. Sample ignition was induced with a 26-gage Nichrome wire coil on top of the upstream edge of the sample under normal ambient pressure as shown in Fig. 2. The igniter is energized using a variable transformer (STACO Energy model 3PN1210B). Once the sample was in position and ignition was achieved, the chamber was sealed to adjust the system to the desired conditions of flow velocity, oxygen concentration and pressure. Two 9000 lumen LED were installed with an operating electronic circuit to act as a strobe light to visualize pyrolysis region and measure flame spread rates and the flame appearance. Each test was video recorded with two different cameras: a Nikon D3200 with a resolution of 1280 by 720 at 59 frames per second and a Sony RX10-III with a resolution of 1920 by 1080 at 120 frames per second. For each test condition, between 4 and 6 experiments were conducted to address the experimental uncertainty.

2.2 Microgravity experiments

Microgravity tests were conducted as part of the BASS-II experiments. The experimental hardware was located inside the Microgravity Science Glovebox (MSG) on board the International Space Station (ISS). This setup provided a contained environment to perform fire experiments while controlling the flow velocity and oxygen concentration. The hardware, shown in Fig. 4, consisted of a flow duct that had a cross section of 76 mm by 76 mm and the length of the test section is 170 mm. A slow forced flow, with velocities ranging between 4 and 80 mm/s, was generated by a small fan at the upstream end of the duct. The flow was then passed through a honeycomb and an inlet screen to reduce swirl. The voltage of the fan was varied to adjust the flow velocity to the desired values, this was check using a hot wire anemometer positioned in between the honeycomb and the inlet screen. The test section had two orthogonal windows that allowed recording of the experiments using two different cameras (Nikon D300 and Panasonic WV-CP654). Inside the test section was a nozzle for nitrogen flow that allowed changing the oxygen concentration between 16% and 21% by volume. Additionally, a radiometer was positioned in the downstream top back corner of the duct to measure flame dynamics and steadiness.

During each test, the PMMA rod was manually ignited by an astronaut with a hot-wire igniter (Kanthal A-1 29 gauge). During ignition, the oxygen concentration was kept constant at a relatively high opposed flow velocity.

Then, the opposed flow was subsequently reduced until extinction, pausing for about 30 s after each reduction to allow for steady propagation at each respective flow velocity. More detailed descriptions of these experiments can be found in [15,33–35].

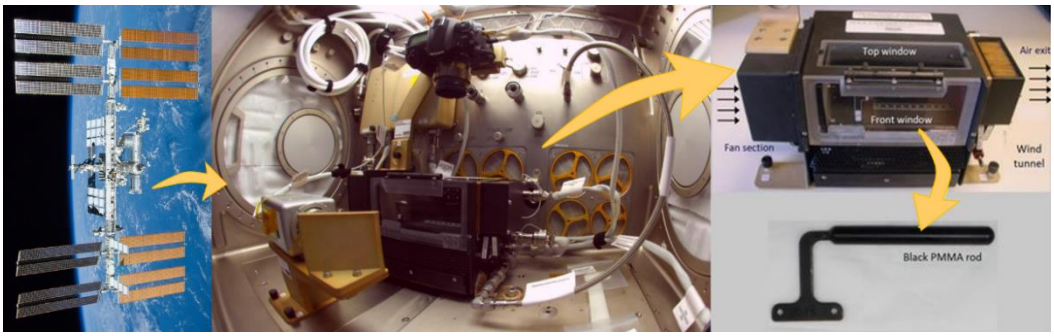

Figure 4. Microgravity experimental apparatus and sample [35].

3 RESULTS

Normal gravity downward flame spread over the PMMA surface was investigated under different ambient pressures and oxygen concentrations. Once ignition was obtained, the flame was observed as it propagated downward over the sample. The rate of spread of the flame was observed to approach steady state soon after the sample was ignited (~ 1 min). Figure 5(a) shows still frames from videos performed in normal gravity at different ambient conditions using the 12.7 mm diameter rod, with a forced flow velocity of 100 mm/s, ambient pressure ranging from 100 to 15 kPa and oxygen concentration from 23% to 19%. Figure 5(b) shows similar frames from videos performed in microgravity using normal ambient pressure and various oxygen concentrations with a forced flow velocity of 15 mm/s, the highest flow velocity tested during BASS-II for the similar rod diameters. For the higher ambient pressures or higher oxygen concentrations, flame tip was very unstable and bright. At these conditions, significant vapor jetting of bubbles of PMMA bursting at the surface is also observed, causing distortions in the flame as the test progressed [36,37]. The flame flickering and vapor jetting appears to decrease as the pressure or oxygen concentration are decreased.

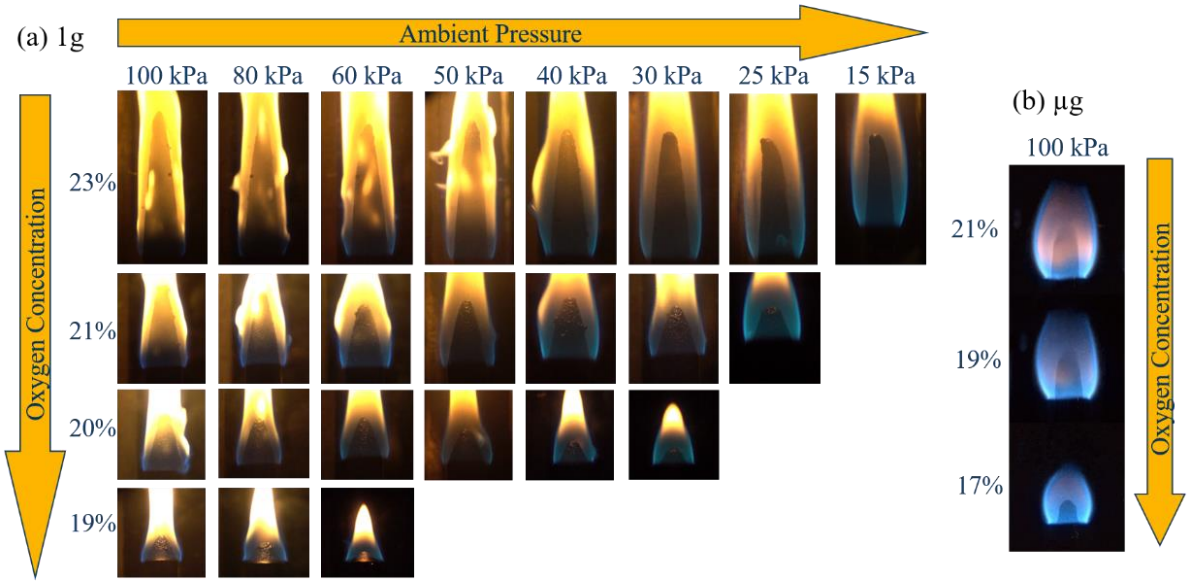

Figure 5. (a) Photo sequence of normal gravity flame appearance in environments with different ambient pressure and oxygen concentration. (b) Photo sequence of microgravity flame appearance in environments with decreasing oxygen concentration at normal ambient pressure. Sample diameter was 12.7 mm.

Figure 5 shows clear differences in flame shape, size and appearance in normal gravity and microgravity. In both environments as oxygen concentration gets reduced the flame becomes smaller. Changes in oxygen concentration affect also the flame color, transitioning form a brighter yellow/orange flame to a dimmer blue flame. Also, in normal gravity, as ambient pressure was reduced the flame size was also reduced, transitioning from a very elongated and tall shape at normal pressure to a more rounded one at reduced pressures. Variation in pressure also affected the flame width, which become larger than the diameter of the sample as pressure was decreased. At the same time, changes in ambient pressure also affected the flame color, with the flame changing from a bright strong yellow to a dimmer blue. This indicates that changes in ambient pressure and oxygen concentration affect soot generation processes and flame temperature, getting reduced with both parameters [38–40]. All these changes experienced by the flame as ambient pressure is decreased result in flames that are more similar to what is observed in microgravity.

The primary data collected from the video recordings was the position of the leading edge of the flame as a function of time, and through it, the downward flame spread rate was obtained. Figure 6 shows the evolution of the flame's leading edge over time for different ambient pressures in air. From the figure, it is possible to see that the spread is fairly steady over time and that as the pressure is reduced the spread of the flame is slower.

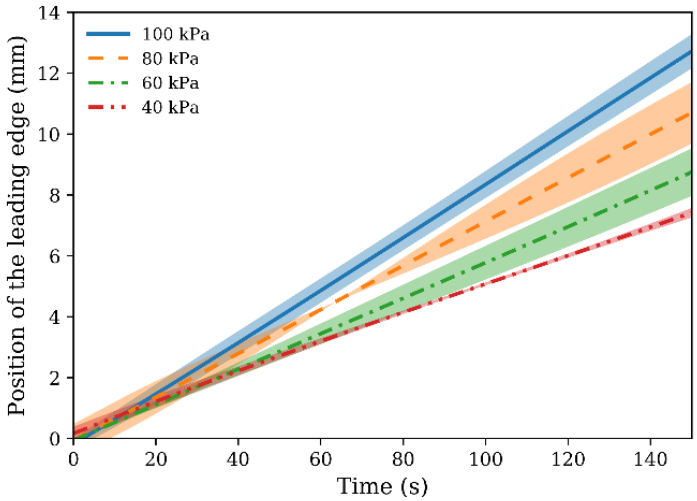

Figure 6. Position of the leading edge of the flame as a function of time for different ambient pressures in air. Cylinder diameter of 12.7 mm

The progress of the flame's leading edge can be used to determine the flame spread rate. The measured flame spread rate as a function of ambient pressure for the 12.7 mm diameter samples is shown in Fig. 7 for the oxygen concentrations tested. Also included in the figure is the data obtained during the BASS experiments at comparable oxygen concentrations and ambient pressure. Figure 8 shows the same data but with the flame spread rate plotted as a function of oxygen concentration and pressure as a parameter. The error from the measurements was calculated as the standard deviation between comparable tests. For all the conditions tested the error was smaller than 8.8%. From Figs. 7 and 8 it is seen that as ambient pressure or oxygen concentration are reduced the flame spread rate is also reduced. Also, notice that the flame spread rate is more sensitive to changes in oxygen concentration than in ambient pressure, with a decrease of 1% oxygen concentration has a similar effect on flame spread rate as that of decreasing ambient pressure from 100 kPa to 40 kPa. Similar observations were made in the work of Ref. [28] for the limiting conditions for flame spread over a thin solid fuel. The flame spread data of Figs. 7 and 8 is also presented in terms of the partial pressure of oxygen in Fig. 9. From Fig. 9 it is seen that the flame spread rate has a linear relation with partial pressure of oxygen.

Comparisons between the normal gravity and microgravity data show that the microgravity data seems to be of comparable magnitude with that observed in normal gravity reduced pressure environment. However, the comparable pressure would also be dependent on the oxygen concentration considered, as flame chemistry is affected by both ambient pressure and oxygen concentration.

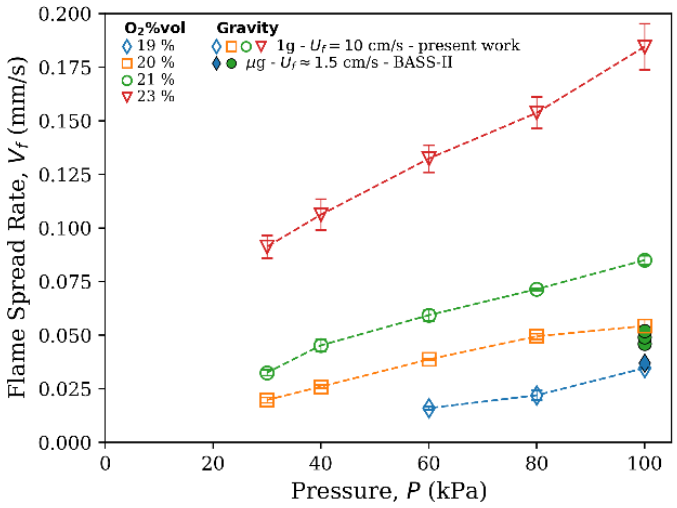

Figure 7. Measured flame spread rate as a function of ambient pressure for different oxygen concentrations. Cylinder diameter of 12.7 mm.

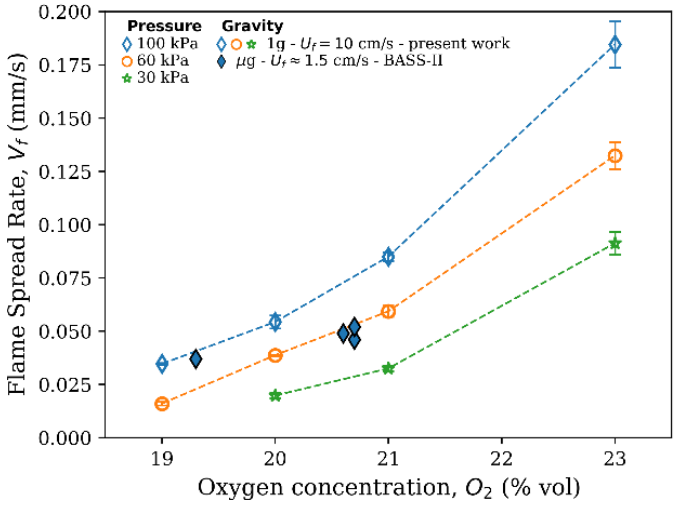

Figure 8. Measured flame spread rate as a function of oxygen concentration for different ambient pressures. Cylinder diameter of 12.7 mm.

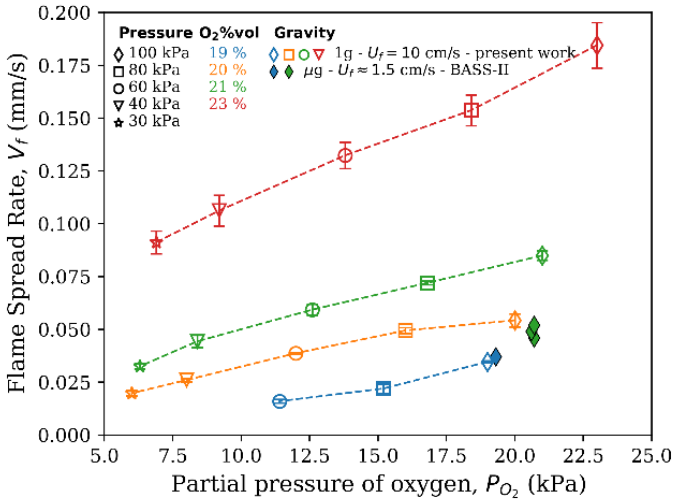

Figure 9. Measured flame spread rate as a function of the partial pressure of oxygen. Cylinder diameter of 12.7 mm.

The variation of the flame spread rate with the sample diameter is shown in Fig. 10, with the flame spreading in 20% oxygen concentration at different ambient pressures. It is seen that as the diameter of the sample is reduced the opposed flow flame spread rate becomes faster, This is due to the heat transfer from the flame to the solid being enhanced by the increase in the curvature of the surface [41] and the reduction of sample thickness. The variation of the spread rate with sample diameter indicates that the rod samples behave more as a thermally thin solid than as thermally thick in terms of the spread of the flame.

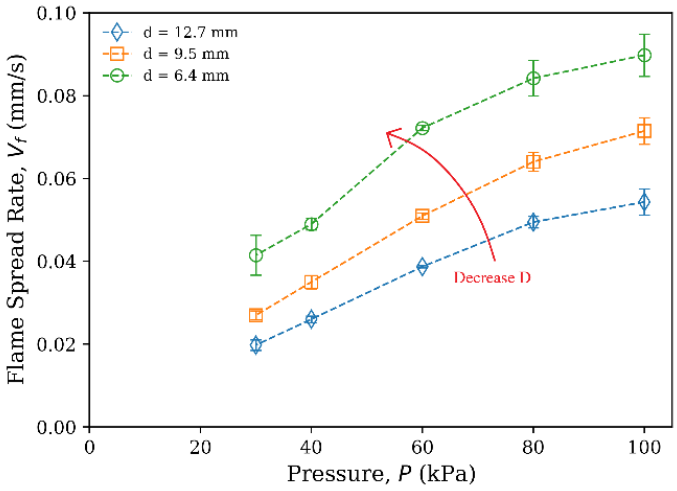

Figure 10. Measured flame spread rate as a function of ambient pressure for diameters 12.7, 9.5, and 6.4 mm. Oxygen concentration was kept constant at 20% by vol.

Downward flame spread for varied ambient pressures and oxygen concentrations has been previously studied for thin materials and the data was correlated as a function of $O_2^{0.9}P^{0.05}$ [42,43]. Following a similar approach, the data of Figs. 7 and 8 was correlated in terms of pressure and oxygen concentration and the results presented in Fig. 11. It is seen that the present data are correlated well with the same pressure and oxygen concentration relation, and that the correlation works fairly well relating not only the normal gravity data but also the microgravity data for all the conditions tested. The correlation shows an almost linear dependence on oxygen concentration and a very weak dependence on pressure.

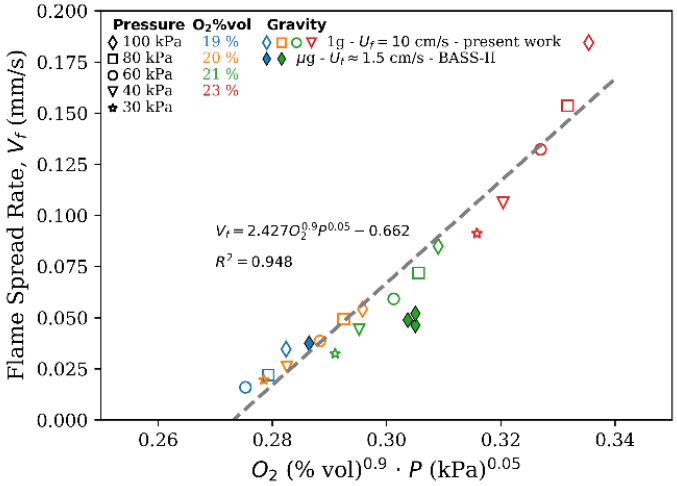

Figure 11. Flame spread rate fit to an oxygen-pressure correlation based on Magee and McAlevy [42]. Cylinder diameter of 12.7 mm.

4 DATA CORRELATION

Although the present experimental data can be correlated with the oxygen-pressure relation presented in Fig. 11, the basis for the correlation is not clear. For this reason, in this section an attempt is made to correlate the data in terms of previously developed theoretical models of opposed flame spread.

The spread of flames over the surface of a solid combustible material is a complex process involving the interaction between the solid phase (heat transfer, thermal decomposition, gasification) and the gas phase (transport, mixing, chemical kinetics) [19,44–46]. In opposed spread, the controlling zones for flame spread and stabilization are located at the flame front. While the thermal length scale is typically small, it controls flame stabilization and forward heat conduction through the gas from the flame. Because the heat flux and the preheat length have the opposite dependence on this length scale, a canceling effect renders the spread of flames over a thin fuel in opposed flow relatively insensitive to the air velocity at low flow velocities [4,19,47,48]. For a thick fuel, however, the ratio of the forward gas phase conduction and the heat conduction into the solid renders the opposed flame spread dependent on the flow velocity [4,19,47,48], increasing as the flow velocity is increased. Flame spread in these conditions is referred as heat transfer controlled. In addition, gas phase chemical kinetics may affect the spread rate tending to reduce the spread as the flow velocity is increased and even cause extinction (blow-off) of the flame at high flow velocities [7,19]. At very low flow velocities in microgravity surface radiation heat losses and chemical kinetic effects (diffusive transport) may also cause extinction (quenching) of the flame [12,49–52]. Thus, although in purely forced flow opposed spread, the downstream flame size (e.g. flame length) does not affect the spread rate significantly, in the presence of gravity the induced flow velocity will increase as the flame becomes larger affecting both the heat transfer from the flame to the solid and the gas phase chemical kinetics.

Despite the complexity of the opposed flame spread processes simplified theoretical models have been developed to determine analytically the flame spread rate. These analyses can be used to correlate the data presented above. Here we will use the simplified analysis of opposed flame spread developed in Refs [19,53], but modified to a cylindrical geometry following the work of Delichatsios [41]. The analysis is based on the concept that flame spread can be viewed as a series of ignition steps where the flame act as the heating and the ignition source [19,44–46]. The analysis provides an analytical expression for the opposed flame spread rate over a solid rod from the ratio of the heating length and the ignition time.

For a thermally thick solid rod it gives:

$$V_f \approx f_{cyl}\left(1-\frac{k_s(T_p-T_\infty)}{\rho_g c_{p,g} U_\infty 2r(T_f-T_p)}\right)^{-1}\frac{l_h(\dot{q}''_{fc}+\dot{q}''_{fr}-\dot{q}''_{rs})^2}{k_s\rho_s c_s\left(T_p-T_o\right)^2}-\varphi\,(Da) \qquad (1)$$

And for a thermally thin fuel:

$$V_f \approx 2f_{cyl}\frac{l_h(\dot{q}''_{fc}+\dot{q}''_{fr}-\dot{q}''_{rs})}{\rho_s c_s r\left(T_p-T_o\right)}-\varphi\,(Da) \qquad (2)$$

where f_{cyl} is a geometrical factor that accounts for the curvature effect of the surface and is defined as

$$f_{cyl}=\frac{c\left(L_g/r\right)}{\ln\left(1+c\frac{L_g}{r}\right)} \qquad (3)$$

In the above equations l_h is the solid heated length upstream of the flame front, $\dot{q}''_{fc}$, represents the convective heat flux from the flame to the solid surface, $\dot{q}''_{fr}$ is the flame radiant flux to the solid surface, $\dot{q}''_{rs}$ the re-radiation from the solid. T_f, T_p and T_∞ represent the flame, pyrolysis and ambient temperature, respectively. ρ_s and c_s are the solid density and specific heat, and k_s, is the solid thermal conductivity. ρ_g and $c_{p,g}$ are the gas density and specific heat. U_∞ is the ambient flow velocity, which includes forced and/or free flow velocity depending of the test conditions. $L_g$is the diffusion length, c is a numerical constant, *r* is the cylinder radius,

and $\varphi\ (Da)$ is a function of the Damkohler number. The first term in Eq. (1) and (2) describes the heat transfer mechanisms of the flame spread process and the second term the gas phase chemical kinetic mechanisms. The chemical kinetics term affects the spread rate at conditions that reduce the Damkohler number and make the term comparable with the heat transfer term. This may occur at low oxygen concentration, low pressure, and at large flow velocity (blow off) [19], or very low flow velocity in microgravity (diffusive transport and radiation losses) [33,52,54,55].

The convective heat flux from the flame to the solid surface can be expressed as, $\dot{q}_c'' = h(T_f - T_p)$, with h representing the convective heat transfer coefficient, T_f the flame temperature and T_p is the PMMA pyrolysis temperature. The flame temperature is directly proportional to the ambient oxygen concentration but is not strongly dependent on ambient pressure until the pressure is relatively low and the chemical time starts to become larger than the physical time. In this work, the flame temperature is assumed to be equal to the adiabatic flame temperature for the different oxygen concentration tested. The radiation from the flame to the solid is generally small in opposed flames spread because of the small view factor [56], and is considered negligible here. The re-radiation from the surface to the surrounding is given by $\dot{q}_{rs}'' = \varepsilon\sigma\left(T_p - T_o\right)$, with ε being the solid emissivity and σ the Stefan-Boltzmann constant.

The heat transfer coefficient is directly related to the boundary layer thickness through $h = k/\delta$. The boundary layer thickness is related to the problem parameters either through the Reynolds number in pure forced flow, or through the Grashof number in pure natural convection (free) flow. For a mixed flow, forced and free, as that of the current normal gravity experiments the boundary layer thickness can be expressed in terms of the Reynolds Number and the Grashof number as [18]

$$\delta_m = Cr[Re^4 + Gr^2]^{-1/8} Pr^{-1/3} \tag{4}$$

Where C is a generic constant related to the type of flow and the rod radius, r, is selected as the characteristic length of the problem, which gives $Re = \frac{\rho_g U_f r}{\mu}$, $Gr = \frac{g\beta\Delta T r^3 \rho_g^2}{\mu^2}$. U_f represents the forced flow velocity component of the mixed flow, μ is the dynamic viscosity, ρ_g is gas phase density, β is the coefficient of thermal expansion and g is the gravity level. Equation (4) shows a general expression for the boundary layer thickness in a mixed flow. Using $h = k/\delta$ together with Eq. (4) and the definitions of the non-dimensional numbers, the mixed flow average convective heat transfer coefficient is given by

$$h_m = \frac{k}{Cr^{1/2}} P^{1/2} U_f^{1/2} \left[1 + \frac{g^2\beta^2\Delta T^2 r^2}{U_f^4}\right]^{1/8} Pr^{1/3} \tag{5}$$

Similarly, a mixed flow gas velocity that would correspond to the actual mixed flow boundary layer at a given set of ambient conditions, i.e. ambient pressure, oxygen concentration, and forced flow velocity, can be determined [37,57]. This mixed flow velocity would be such that if applied in a pure forced flow, would produce a similar heat transfer coefficient as that of Eq. (5). Solving for the flow velocity in the forced flow boundary layer, the following mixed convection velocity, U_m, is obtained in terms of pressure, forced flow velocity in the mixed flow, and gravity.

$$U_m = \frac{P}{P_0}\left[U_f^4 + g^2\beta^2\Delta T^2 r^2\right]^{1/4} \tag{6}$$

where P_0 is a reference ambient pressure (standard Earth ambient pressure) and U_f is the forced flow velocity at this reference pressure P_0. From Eq. (6) it is seen that for zero gravity or large flow velocity the mixed flow velocity is that of a pure forced flow at a given test pressure, $U_m = \frac{P}{P_0} U_f$. For elevated gravity and/or zero forced velocity, the mixed flow velocity becomes that of natural convection at a given test pressure and oxygen concentration, $U_m = \frac{P}{P_0}(g\beta\Delta T r)^{\frac{1}{2}}$. Thus, it would be possible to approximately predict the flame spread rate in a pure forced flow, as that experienced in micro-gravity, with a normal gravity test that has a similar mixed

convection boundary layer as that of the forced flow, or conversely. In this case, the convective heat transfer coefficient for the forced flow, based on the mixed flow velocity, would be

$$h = C\frac{k}{r}\left(\frac{U_m Pr}{\mu}\right)^{1/2} Pr^{1/3} \tag{7}$$

and the convective heat flux from the flame to the solid ahead of it can be approximately expresses as

$$\dot{q}_c'' = C\frac{k}{r}\left(\frac{U_m Pr}{\mu}\right)^{1/2} Pr^{1/3}(T_f - T_p) \tag{8}$$

The solid heated length, l_h, correspond to the portion of unburned fuel ahead of the leading edge of the flame that is heated by the flame radiation and convection through the gas, and conduction through the solid. In opposed flame spread, the heated length can be scaled as the boundary layer thickness, so for a forced flow condition $l_h \sim \delta \sim rRe^{-1/2} \sim \left(\mu r/\rho_g U_\infty\right)^{1/2}$ [53]. Applying these approximations to the flame spread expressions of Eq. (1) and (2) the following expressions are obtained for the flame spread rate for a thermally thick solid

$$V_f \approx Cf_{cyl}\left(1 - \frac{k_s(T_p - T_\infty)}{\rho_g c_{p,g} U_\infty 2r(T_f - T_p)}\right)^{-1}\left(\frac{\mu r}{PU_m}\right)^{\frac{1}{2}} \frac{\left(\frac{k}{r}\left(\frac{U_m Pr}{\mu}\right)^{\frac{1}{2}} Pr^{\frac{1}{3}}(T_f - T_p) - \dot{q}_{rs}''\right)^2}{k_s\rho_s c_s(T_p - T_o)^2} - \varphi(Da) \tag{9}$$

And for a thermally thin fuel

$$V_f \approx 2f_{cyl}\left(\frac{\mu r}{PU_m}\right)^{\frac{1}{2}} \frac{\left(\frac{k}{r}\left(\frac{U_m Pr}{\mu}\right)^{\frac{1}{2}} Pr^{\frac{1}{3}}(T_f - T_p) - \dot{q}_{rs}''\right)}{\rho_s c_s r(T_p - T_o)} - \varphi\,(Da) \tag{10}$$

It should be noted that the first term in Eq. (9) and (10) without the reradiation heat flux, is basically the same to those previously developed in Refs. [41,47,48,58] in different analyses of opposed flame spread.

Since the rod samples used in these experiments have an intermediate thickness between thermally thin and thick for flame spread purposes (Fig. 10), from Eqs. (9) and (10) it is inferred that the flame spread may be a function of the opposed flow velocity. This can be verified by plotting the flame spread rate data of Figs. 7 and 8 in terms of the mixed flow velocity, U_m, with the ambient pressure and oxygen concentration as parameters, as it is shown in Fig. 12. Error of the 1g measurements was smaller than 8.8%. The results predict a spread rate that increases approximately linearly with the mixed flow velocity suggesting that the spread rate occurs primarily in the thermal regime for the conditions tested.

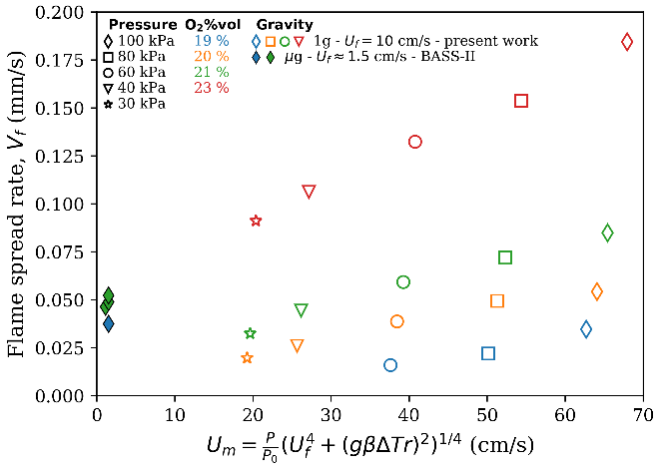

Figure 12. Measured flame spread rate as a function of the mixed flow velocity, U_m, obtained from Eq. (6).

Extrapolating the data in Fig. 12 to zero flame spread shows that for a given oxygen concentration there is a limiting flow velocity below which no flame spread occurs, with the velocity increasing as the oxygen concentration decreases. Similarly, at a given pressure, reducing the oxygen concentration there is a limiting flow velocity for flame spread to occur. This indicates that the spread rate is a function of the mixed flow velocity and the oxygen concentration as predicted by Eqs. (9) and (10) but with limiting values for flame spread at certain flow velocities and oxygen concentrations. With these considerations, the data of Fig. 12 can be correlated in terms of the flow velocity and oxygen concentration as shown in Fig. 13. It is seen that the flame spread rate data in normal gravity is correlated fairly well with the flame spread expression of Fig. 13, but the microgravity data not so well. It should be kept in mind, however, that the microgravity data was obtained at very low flow velocities (~1.5 cm/s), where a boundary layer analysis as that used in this work to calculate the convective heat flux and correlate the data may not be fully applicable. At these very low velocity flows, diffusion transport might become more relevant for the flame spread process when compared to the forced flow. In this case, the actual flow velocity that the flame would be exposed to would be approximately the sum of the forced flow velocity and the diffusion velocity, which would bring the microgravity data closer to the correlation. Furthermore, it may also be due to the different flow characteristics between the flow in microgravity and the mixed flow in normal gravity. The former would be primarily parallel to the rod surface while the later may have a component perpendicular to the surface driven by the buoyant flow.

From the correlation of Fig. 13 two constants arise, O_0 and U_0. The first one, O_0 can be viewed as a limiting oxygen concentration below which the flame cannot spread due to chemical kinetic effects. This limiting oxygen concentration seems to be similar to the limiting oxygen concentration (LOC) for flame spread [59]. The second one, U_0, can be related to a limiting flow velocity below which the flame will not be able to spread. This limit seems to be related to a radiation balance or diffusion transport limit [49–52].

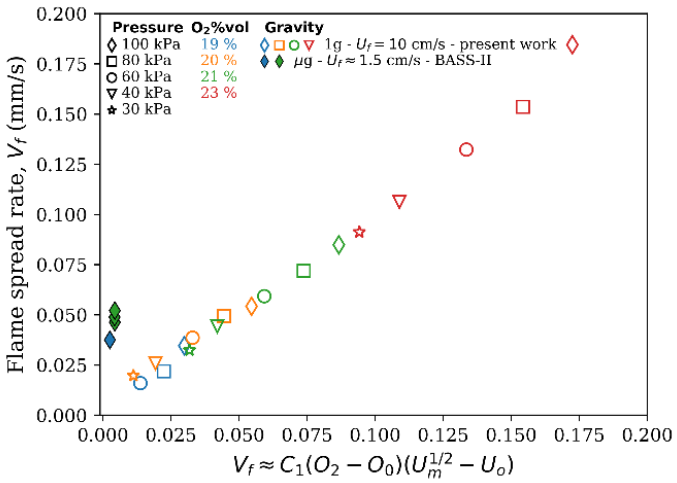

Figure 13. Measured flame spread rate correlated in terms of oxygen concentration, O_2, and the squared root of the mixed flow velocity, U_m

Furthermore, since T_f is directly proportional to O_2, the correlation of Fig. 13 can be modified in terms of T_f as predicted in the theoretical analysis leading to Eqs. (9) and (10). This is done in Fig. 14. The results from this figure show that the opposed flame spread can be correlated well by a relation that includes two primary parameters: one that describes the convective heat transfer from the flame to the solid $\left(C_1 U_m^{1/2}(T_f - T_p)\right)$ and another that describes the gas phase chemical effects $\left(f(U_m, T_f, T_p) = -C_1 U_0 (T_f - T_p) - C_2 (U_m^{1/2} - U_0)\right)$. Note that this correlation predicts a dependence on the flow velocity that corresponds to a thermally thick solid (Eq. 9), while the dependence on the flame temperature corresponds to a thermally thin material (Eq.10). In addition, the term $f(U_m, T_f, T_p)$ corresponds to the chemical kinetic component, $\varphi(Da)$ in Eqs. (9) or (10). Although these results seem to imply that the rods used in this work are not thermally thick or thin, it may also

imply that the gas flow characteristics do not correspond to a parallel boundary layer flow, as assumed to obtain the heat flux in Esq. (7) and (8). In a vertical surface the buoyant flow driven by a downward spreading flame has a perpendicular component that may change the heat transfer from the flame to the solid. This would change the flame spread rate predictions of Eqs. (9) and (10). The authors are unaware of an analytical expression for the resulting heat transfer coefficient and a numerical analysis is beyond the scope of this work.

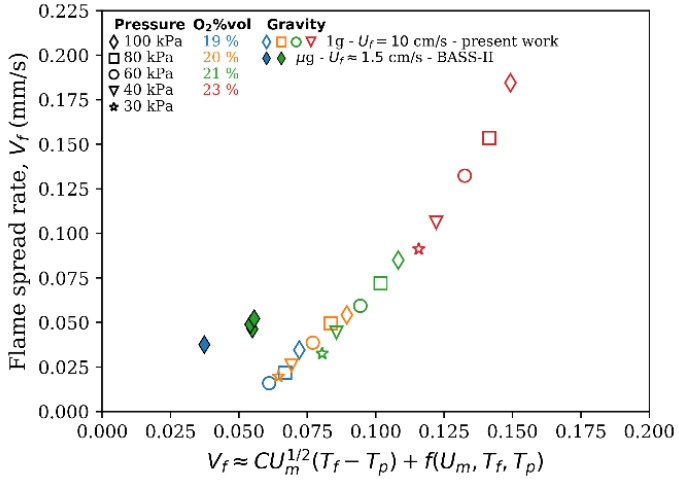

Figure 14. Average flame spread rate correlated in terms of flame temperature, $T_f \sim O_2$, and the squared root of the mixed flow velocity, U_m.

The correlation presented here includes the effects of ambient pressure, or buoyancy, oxygen concentration, and gravity, and depending on these conditions the dominant regime in the spread process can change from a thermally controlled regime to a chemical kinetic controlled regime, and vice versa. For large Damkohler numbers, i.e. high oxygen concentration, high pressure, and low velocity flows, the reaction rate is very fast and gas phase chemistry becomes less important when compared with the heat being transferred to the solid material. For smaller values of Damkohler number, given particularly at low oxygen concentrations, low pressure, and large flow velocities, the reaction rate is much slower. At these conditions, the chemical time becomes larger than the residence time, the gas phase chemical reactions become important and rate of spread of the flame over the solid is mainly controlled by how fast the fuel is consumed. Given the conditions of the present experiments, it is necessary to consider both effects. The present flow velocities are fairly small to affect chemical effects (far away from blow off), at least at the elevated ambient pressures and high oxygen concentration where chemistry is not dominant. However, as ambient pressure and oxygen concentration are reduced the reaction rate is reduced, and the chemical time increases accordingly, giving more importance to the $\varphi(Da)$ term. The work of McAllister et al. [60] showed that chemical kinetics effects would not affect ignition of PMMA in air until the ambient pressure was smaller than 30 kPa. However, this result is strongly dependent on oxygen concentration, and the ambient pressure at which chemistry becomes important will increase as the oxygen concentration is reduced and approaches the limiting oxygen concentration, (LOC 17.1% O_2 [59]).

It should also be noted that since U_m is dependent on the gravity level, as shown in Eq. (6), it is possible to obtain a relation between the gravity level and the mixed flow velocity, which in turn can be used to predict flame spread at different gravity levels. This relation is presented in Eq. (11) and relates changes in ambient pressure to different gravity levels through the mixed flow velocity.

$$g = \frac{1}{r(\beta \Delta T)}\left[\left(\frac{U_{mP_0}}{P}\right)^4 - U_f^4\right]^{1/2} \tag{11}$$

Thus Eq. (11) together with Eq. (6) can be used to predict the flame spread rate at different gravity levels such as those of the Moon or Mars.

5 CONCLUSIONS

The opposed flame spread rate and flame appearance over PMMA cylinders has been studied under reduced ambient pressure and variable oxygen concentration to determine the effect of buoyancy on the opposed flame spread process. Future spacecraft environments that may include reduce ambient pressure and increased oxygen concentration are also a motivation for the study. It has been found that as pressure or oxygen concentration is reduced, the flame spread rate over the surface of the PMMA rods is also reduced. Flame intensity and length are also reduced, resulting in rounder and dimmer blue flames for the lowest pressures. As ambient pressure is progressively decreased, the flame spread characteristics get closer to what is observed in microgravity.

The normal gravity flame spread rate data can be correlated well in terms of a product of pressure and oxygen concentration functions that are derived from analytical formulas of opposed flame. The correlations suggest that the rods tested may behave between thermally thick and thermally thin, and that the behavior may depend on the levels of oxygen concentration and pressure. The microgravity data is not correlated as well probably because the microgravity data was obtained at very low flow velocities (~1.5 cm/s), and the boundary layer analysis used for the correlation may not apply. Another possibility is that the characteristics of the flow in microgravity may be somewhat different than the flow generated by flame buoyancy. This may indicate that simulating opposed flow flame spread in microgravity by reducing pressure, may produce approximate results only. Furthermore, it should also be kept in mind that reducing ambient pressure will eventually affect flame chemistry. Thus, caution should be taken in extrapolating low ambient pressure data to predict flame spread at different gravity levels.

Also, worth noting is that at different gravity levels, such as on the Moon or Mars, the opposed flame spread can be predicted by reducing the pressure so that the mixed flow gas velocity remains the same than that at reduced gravity. At those intermediate gravity levels, the simulation pressure would be higher, and the chemical kinetic effects could be reduced.

ACKNOWLEDGMENTS

This work was supported by NASA Grants NNX10AE01G and NNX13AL10A. The authors would like to acknowledge the invaluable assistance of all the astronauts who ran BASS-II. We also want to acknowledge the efforts of the BASS ops team, and the ground support teams at GRC, JSC, and MSFC. Also, the authors would like to thank Grace Mendoza, Madison Hales, Runbiao Wei, Ryan So, Christina Liveretou, and Mina Fanaian for their assistance conducting the experiments.

REFERENCES

[1] R. Friedman, Fire Safety in Spacecraft, Fire Mater. 20 (1996) 235–243.

[2] H.D. Ross, Microgravity combustion : fire in free fall, Academic Press, 2001.

[3] G. Jomaas, J.L. Torero, C. Eigenbrod, J. Niehaus, S.L. Olson, P. V Ferkul, G. Legros, A.C. Fernandez-Pello, A.J. Cowlard, S. Rouvreau, N. Smirnov, O. Fujita, J.S. T 'ien, G.A. Ruff, D.L. Urban, Fire safety in space – beyond flammability testing of small samples, Acta Astronaut. 109 (2015) 208–216. doi:10.1016/j.actaastro.2014.11.025.

[4] J.G. Quintiere, Fundamental of Fire Phenomena, John Wiley, New York, 2006.

[5] K.E. Lange, A.T. Perka, B.E. Duffield, F.F. Jeng, Bounding the Spacecraft Atmosphere Design Space for Future Exploration Missions, 2005. http://ntrs.nasa.gov/search.jsp?R=20050185597.

[6] P.D. Campbell, Recommendations for Exploration Spacecraft Internal Atmospheres, Houston, Texas, 2006.

[7] C. Fernandez-Pello, S.R. Ray, I. Glassman, Flame spread in an opposed forced flow: the effect of ambient oxygen concentration, Symp. Combust. 18 (1981) 579–589. doi:10.1016/S0082-

0784(81)80063-X.
[8] K.R. Sacksteder, J.S. Tien, Buoyant downward diffusion flame spread and extinction in partial-gravity accelerations, Twenty-Fifth Symp. Coinbustion/The Combust. Institute,. (1994) 1685–1692.
[9] M. Kikuchi, O. Fujita, K. Ito, A. Sato, T. Sakuraya, Experimental study on flame spread over wire insulation in microgravity, Symp. Combust. 27 (1998) 2507–2514. doi:10.1016/S0082-0784(98)80102-1.
[10] F. Higuera, A. Liñán, Flame spread along a fuel rod in the absence of gravity, Combust. Theory Model. 3 (1999) 259–265. doi:10.1088/1364-7830/3/2/003.
[11] M. Roslon, S. Olenick, Y.Y. Zhou, D.C. Walther, J.L. Torero, A.C. Fernandez-Pello, H.D. Ross, Microgravity Ignition Delay of Solid Fuels in Low-Velocity Flows, AIAA J. 39 (2001) 2336–2342. doi:10.2514/2.1239.
[12] S.L. Olson, U. Hegde, S. Bhattacharjee, J.L. Deering, L. Tang, R.A. Altenkirch, Sounding rocket microgravity experiments elucidating diffusive and radiative transport effects on flame spread over thermally thick solids, Combust. Sci. Technol. 176 (2004) 557–584. doi:10.1080/00102200490276773.
[13] S. Olson, G. Ruff, Microgravity Flame Spread over Non-Charring Materials in Exploration Atmospheres: Pressure, Oxygen, and Velocity Effects on Concurrent Flame Spread, SAE Tech. Pap. 2009-01-2489. (2009). doi:10.4271/2009-01-2489.
[14] S. Bhattacharjee, R. Ayala, K. Wakai, S. Takahashi, Opposed-flow flame spread in microgravity-theoretical prediction of spread rate and flammability map, Proc. Combust. Inst. 30 (2005) 2279–2286. doi:10.1016/j.proci.2004.08.020.
[15] S.L. Olson, P. V Ferkul, S. Bhattacharjee, F.J. Miller, A.C. Fernandez-Pello, J.S. T'ien, Burning and Suppression of Solids – II Fire Safety Investigation for the Microgravity Science Glovebox, in: 29th Annu. Meet. Am. Soc. Gravitational Sp. Res. 5th Int. Symp. Phys. Sci. Sp., Orlando, FL, 2013.
[16] D.L. Urban, P. Ferkul, S. Olson, G.A. Ruff, J.S. T'ien, Y.T. Liao, A.C. Fernandez-pello, J.L. Torero, G. Legros, C. Eigenbrod, N. Smirnov, O. Fujita, S. Rouvreau, B. Toth, G. Jomaas, Flame Spread : Effects of Microgravity and Scale, Combust. Flame. 199 (2019) 168–182. doi:10.1016/j.combustflame.2018.10.012.
[17] D. Drysdale, Introduction to Fire Dynamics, Wiley, 1998.
[18] C.-P. Mao, A.C. Fernandez-Pello, P.J. Pagni, Mixed convective buring of a fuel surface with arbitrary inclination, J Heat Transf. 106 (1984) 304–309. doi:10.1115/1.3246673.
[19] C. Fernandez-pello, The solid phase, in: G. Cox (Ed.), Combust. Fundam. Fire, Academic Press Limited, 1994: pp. 31–100.
[20] X. Chen, J. Liu, Z. Zhou, P. Li, T. Zhou, D. Zhou, J. Wang, Experimental and theoretical analysis on lateral flame spread over inclined PMMA surface, Int. J. Heat Mass Transf. 91 (2015) 68–76. doi:10.1016/j.ijheatmasstransfer.2015.07.072.
[21] D.D. Drysdale, A.J.R. Macmillan, Flame spread on inclined surfaces, Fire Saf. J. 18 (1992) 245–254. doi:10.1016/0379-7112(92)90018-8.
[22] M.J. Gollner, C.H. Miller, W. Tang, A. V. Singh, The effect of flow and geometry on concurrent flame spread, Fire Saf. J. 91 (2017) 68–78. doi:10.1016/j.firesaf.2017.05.007.
[23] M.J. Gollner, X. Huang, J. Cobian, A.S. Rangwala, F.A. Williams, Experimental study of upward flame spread of an inclined fuel surface, Proc. Combust. Inst. 34 (2013) 2531–2538. doi:10.1016/j.proci.2012.06.063.
[24] L. Zhou, A.C. Fernandez-Pello, Turbulent, concurrent, ceiling flame spread: The effect of buoyancy, Combust. Flame. 92 (1993) 45–59. doi:10.1016/0010-2180(93)90197-B.
[25] H.T. Loh, C. Fernandez-Pello, A study of the controlling mechanisms of flow assisted flame spread, Twent. Symp. Combust. Combust. Inst. (1984) 1575–1582.
[26] C. Fernandez-pello, C.-P. Mao, A Unified Analysis of Concurrent Modes of Flame Spread, Combust. Sci. Technol. 26 (1981) 147–155. doi:10.1080/00102208108946954.
[27] S.H. Chung, C.K. Law, An experimental study of droplet extinction in the absence of external convection, Combust. Flame. 64 (1986) 237–241. doi:10.1016/0010-2180(86)90061-1.

[28] M. Thomsen, D.C. Murphy, C. Fernandez-pello, D.L. Urban, G.A. Ruff, Flame spread limits (LOC) of fire resistant fabrics, Fire Saf. J. 91 (2017) 259–265. doi:10.1016/j.firesaf.2017.03.072.
[29] Y. Nakamura, N. Yoshimura, H. Ito, K. Azumaya, O. Fujita, Flame spread over electric wire in sub-atmospheric pressure, Proc. Combust. Inst. 32 (2009) 2559–2566. doi:10.1016/j.proci.2008.06.146.
[30] J. Kleinhenz, I.I. Feier, S.Y. Hsu, J.S. T'ien, P. V. Ferkul, K.R. Sacksteder, Pressure modeling of upward flame spread and burning rates over solids in partial gravity, Combust. Flame. 154 (2008) 637–643. doi:10.1016/j.combustflame.2008.05.023.
[31] S. Fereres, C. Fernandez-Pello, D.L. Urban, G.A. Ruff, Identifying the roles of reduced gravity and pressure on the piloted ignition of solid combustibles, Combust. Flame. 162 (2015) 1136–1143. doi:10.1016/j.combustflame.2014.10.004.
[32] R.A. Altenkirch, R. Eichhorn, P.C. Shang, Buoyancy effects on flames spreading down thermally thin fuels, Combust. Flame. 37 (1980) 71–83. doi:10.1016/0010-2180(80)90072-3.
[33] S. Bhattacharjee, A. Simsek, F. Miller, S. Olson, P. Ferkul, Radiative, thermal, and kinetic regimes of opposed-flow flame spread: A comparison between experiment and theory, Proc. Combust. Inst. 36 (2017) 2963–2969. doi:10.1016/j.proci.2016.06.025.
[34] S.L. Olson, P. V. Ferkul, Microgravity flammability boundary for PMMA rods in axial stagnation flow: Experimental results and energy balance analyses, Combust. Flame. 180 (2017) 217–229. doi:10.1016/j.combustflame.2017.03.001.
[35] S. Link, X. Huang, C. Fernandez-Pello, S. Olson, P. Ferkul, The Effect of Gravity on Flame Spread over PMMA Cylinders, Sci. Rep. 8 (2018) 120. doi:10.1038/s41598-017-18398-4.
[36] C. Eigenbrod, G. Ruff, S.L. Olson, P. V. Ferkul, Experimental Results on the Effect of Surface Structures on the Flame Propagation Velocity of PMMA in Microgravity Experimental Results on the Effect of Surface Structures on the Flame Propagation Velocity of PMMA in Microgravity, in: 47th Int. Conf. Environ. Syst., Charleston, SC, 2017: pp. 1–11.
[37] M. Thomsen, C. Fernandez-Pello, G.A. Ruff, D.L. Urban, Buoyancy effects on concurrent flame spread over thick PMMA, Combust. Flame. 199 (2019) 279–291. doi:10.1016/j.combustflame.2018.10.016.
[38] A. Fuentes, G. Legros, A. Claverie, P. Joulain, J.P. Vantelon, J.L. Torero, Interactions between soot and CH* in a laminar boundary layer type diffusion flame in microgravity, Proc. Combust. Inst. 31 II (2007) 2685–2692. doi:10.1016/j.proci.2006.08.031.
[39] G. Legros, J.L. Torero, Phenomenological model of soot production inside a non-buoyant laminar diffusion flame, Proc. Combust. Inst. 35 (2015) 2545–2553. doi:10.1016/j.proci.2014.05.038.
[40] J. Citerne, H. Dutilleul, K. Kizawa, M. Nagachi, O. Fujita, M. Kikuchi, G. Jomaas, S. Rouvreau, J.L. Torero, G. Legros, Acta Astronautica Fire safety in space – Investigating flame spread interaction over wires, Acta Astronaut. 126 (2016) 500–509. doi:10.1016/j.actaastro.2015.12.021.
[41] M.A. Delichatsios, R.A. Altenkirch, M.F. Bundy, S. Bhattacharjee, L.I.N. Tang, K. Sacksteder, Creeping flame spread along fuel cylinders in forced and natural flows and microgravity, Proc. Combust. Inst. 28 (2000) 2835–2842.
[42] R.S. Magee, R.. McAlevy III, The Mechanisms of Flame Spread, J. Fire Flammabl. 2 (1971) 271–297.
[43] S.L. Olson, G.A. Ruff, F.J. Miller, Microgravity Flame Spread in Exploration Atmospheres: Pressure, Oxygen, and Velocity Effects on Opposed and Concurrent Flame Spread, in: 38th Int. Conf. Environ. Syst., San Francisco, California, 2008: pp. 1–8. doi:10.4271/2008-01-2055.
[44] F.A. Williams, Mechanisms of fire spread, Symp. Combust. 16 (1976) 1281–1294. doi:10.1016/S0082-0784(77)80415-3.
[45] J. Quintiere, A simplified theory for generalizing results from a radiant panel rate of flame spread apparatus, Fire Mater. 5 (1981) 52–60. doi:10.1002/fam.810050204.
[46] M.A. Delichatsios, Creeping flame spread: energy balance and application to practical materials, Symp. Combust. 26 (1996) 1495–1503.
[47] J.N. De Ris, Spread of a laminar diffusion flame, Symp. Combust. 12 (1969) 241–252. doi:10.1016/S0082-0784(69)80407-8.
[48] I.S. Wichman, Theory of opposed-flow flame spread, Prog. Energy Combust. Sci. 18 (1992) 553–593.

doi:10.1016/0360-1285(92)90039-4.
[49] J.S. T'ien, Diffusion Flame Extinction at Small Stretch Rates : The Mechanism of Radiative Loss, Combust. Flame. 4 (1986) 31–34.
[50] S.L. Olson, Mechanisms of Microgravity Flame Spread Over a Thin Solid Fuel: Oxygen and Opposed Flow Effects, Combust. Sci. Technol. 76 (1991) 233–249. doi:10.1080/00102209108951711.
[51] S. Bhattacharjee, K. Wakai, S. Takahashi, Predictions of a critical fuel thickness for flame extinction in a quiescent microgravity environment, Combust. Flame. 132 (2003) 523–532. doi:10.1016/S0010-2180(02)00501-1.
[52] S. Takahashi, M. Kondou, K. Wakai, S. Bhattacharjee, Effect of radiation loss on flame spread over a thin PMMA sheet in microgravity, Proc. Combust. Inst. 29 (2002) 2579–2586.
[53] A.C. Fernandez-pello, Modelling flame spread as a flame induced solid ignition process, Fire Explos. Hazards Proc. Fourth Int. Semin. (2004) 13–26.
[54] S.L. Olson, P. V. Ferkul, J.S. T'ien, Near-limit flame spread over a thin solid fuel in microgravity, Symp. Combust. 22 (1988) 1213–1222. doi:10.1016/S0082-0784(89)80132-8.
[55] Y.-T. Tseng, J.S. T'ien, Limiting Length, Steady Spread, and Nongrowing Flames in Concurrent Flow Over Solids, J. Heat Transfer. 132 (2010) 091201. doi:10.1115/1.4001645.
[56] A.C. Fernandez-Pello, R.J. Santoro, On the dominant mode of heat transfer in downward flame spread, Symp. Combust. 17 (1979) 1201–1209. doi:10.1016/S0082-0784(79)80114-9.
[57] M. Thomsen, C. Fernandez-pello, D.L. Urban, G.A. Ruff, S.L. Olson, On simulating concurrent flame spread in reduced gravity by reducing ambient pressure, Proc. Combust. Inst. 37 (2019) 3793–3800.
[58] S. Bhattacharjee, S. Takahashi, K. Wakai, C.P. Paolini, Correlating flame geometry in opposed-flow flame spread over thin fuels, Proc. Combust. Inst. 33 (2011) 2465–2472. doi:10.1016/j.proci.2010.06.053.
[59] D. Hirsch, S. Motto, A. Porter, H. Beeson, M.D. Pedley, Issues related to the flammability assessment of polymers for hazard analyses of oxygen systems, Flammabl. Sensit. Mater. Oxyg. Enriched Atmos. 10th Vol. ASTM Int. (2003).
[60] S. McAllister, C. Fernandez-Pello, D. Urban, G. Ruff, The combined effect of pressure and oxygen concentration on piloted ignition of a solid combustible, Combust. Flame. 157 (2010) 1753–1759. doi:10.1016/j.combustflame.2010.02.022.